IEEE Photonics Journal
An IEEE Photonics Society Publication

Open Access

Simulation for Optical Response of High-Speed Traveling Wave Electro-Optic Polymer/TiO_2 Multilayer Slot Waveguide Modulators

Volume 9, Number 3, June 2017

Dan Zhang, *Member, IEEE*
Yasufumi Enami, *Member, IEEE*

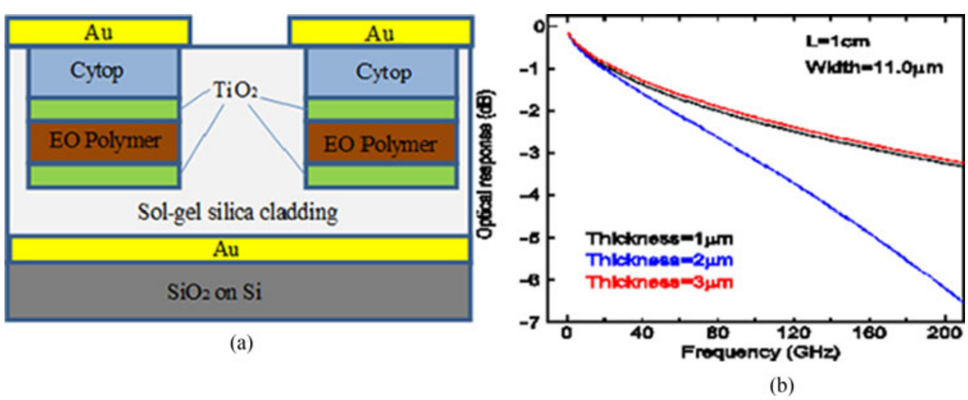

DOI: 10.1109/JPHOT.2017.2700870
1943-0655

Simulation for Optical Response of High-Speed Traveling Wave Electro-Optic Polymer/TiO_2 Multilayer Slot Waveguide Modulators

Dan Zhang,[1] ***Member, IEEE*****, and Yasufumi Enami,**[2] ***Member, IEEE***

[1]College of Information Science and Technology, Nanjing Forestry University, Nanjing 210037, China
[2]Graduate School of Engineering, Kochi University of Technology, Kami, Kochi 782-8502, Japan

DOI:10.1109/JPHOT.2017.2700870

Manuscript received March 22, 2017; revised April 28, 2017; accepted May 1, 2017. Date of publication May 3, 2017; date of current version May 19, 2017. Corresponding author: Dan Zhang (e-mail: zhangdan1227@hotmail.com).

Abstract: In this paper, we analyze a traveling wave electrode as it drives a high-speed electro-optic (EO) polymer/TiO_2 multilayer slot waveguide modulator by simulation. To enhance its mode confinement, the EO polymer is clipped by TiO_2 slot waveguide films, and the electrode atop the active region and connection transmission line are optimized to match the impedance at 50 Ω. The optical response is over 200 GHz at 3-dB bandwidth with a 1-cm-long electrode. By comparison, the optical response with silicon TiO_2 layers is only 20 GHz with transverse electric (TE) polarized light.

Index Terms: Electro-optic (EO) polymer modulator, traveling wave electrode, polymer modulator, slot waveguide.

1. Introduction

Researchers and developers have generated considerable interest in electro-optic (EO) polymer modulators over the past several years because they exhibit wide bandwidth, low drive power, and polarization-independent operation [1]–[3]. To be specific, they exhibit electronic bandwidths up to 113 GHz for optical response of 3-dB due to low dielectric dispersion (less than one tenth the dispersion of semiconductors and $LiNbO_3$). [3]. EO polymers and silicon optical modulators can be integrated easily with most widely commercialized complementary metal-oxide-semi-conductor (CMOS) circuits; however, there is excessive optical absorption loss in the Si-EO polymer modulator. For example, in the Si-EO polymer coplanar slot ring resonator waveguide of a modulator, the lowest value reported is 35 dB/cm [4]. To suit practical applications, they must be further optimized.

When the TiO2 thin layer is used with an EO polymer layer, the effective field is strengthened in the EO polymer layer and may cause a reduction in switching voltage as the dielectric constant of TiO2 is higher than that of the EO polymer. The goal of this study was to build a favorable EO polymer/TiO_2 multilayer slot waveguide modulator. To test the potential of EO polymers for 3-dB bandwidths, we used metallic upper and lower electrodes and measured the lower half-wave voltage at 1 kHz [5], [6]. To effectively realize 3-dB bandwidths at more than 100 GHz for

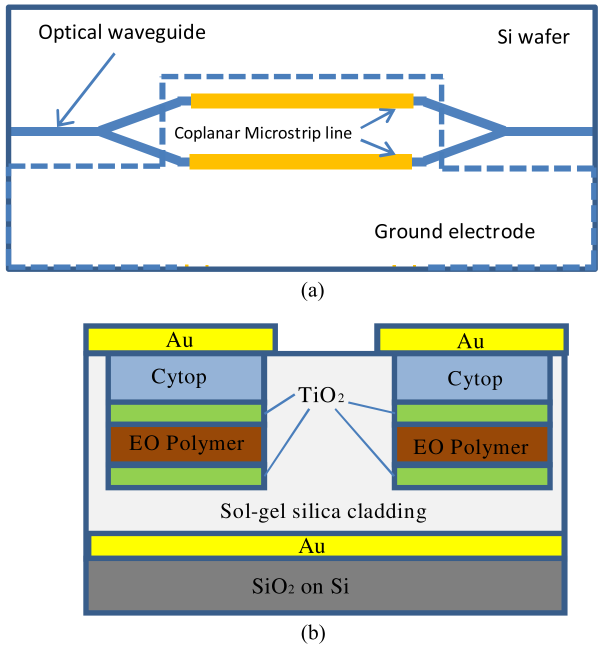

Fig. 1. Top and cross-sectional views of EO polymer/TiO2 multilayer slot waveguide modulator active region. (a) Top-sectional view. (b) Cross-sectional view.

future high-speed applications, however, electrodes that function at gigahertz frequency bands are necessary.

The traveling wave electrodes have been considered to be used in high speed operation of integrated electro-optic Mach-Zehnder interferometer modulators [7]. The first demonstrations of traveling wave Mach-Zehnder polymer modulators were in the early 1990s [8], [9], and the first 100 GHz operation phase modulator was reported by the UCLA/USC groups [1]. Within the limits of our knowledge, up to present, 2 cm length with RF bandwidth of ~20 GHz and 1 cm device with RF bandwidth of ~40 GHz intensity modulator have been reported at the beginning of this century [10]. The bandwidth of an EO modulator built with a traveling-wave electrode is limited by mismatched velocity between the microwave and optical mode in addition to the RF transmission loss of the electrode. The modulation bandwidth of polymer modulators is limited by electrode transmission characteristics due to the intrinsically low dielectric constant of EO polymers. Suitable traveling-wave electrode thickness can reduce the microwave transmission loss, however, while providing the required velocity match for wideband operation.

Characteristic electrode impedance affects both frequency response and driving power. It is essential to ensure impedance matching among the electrode, drive circuit, and terminating load to reduce microwave reflections at each end of an electrode; this is the fundamental concept of the traveling wave electrode, where the electrode represents an extension of the driving transmission line. The electrode should have the same characteristic impedance as the driving source (50 Ω), accordingly.

Modern devices contain two main types of traveling-wave electrodes: Coplanar microstrip line (CPS) electrodes [9] and coplanar waveguide (CPW) electrodes [7], [11]. A CPS electrode generally has lower transmission loss and lower driving voltage for a directional coupler modulator compared to a CPW electrode. The transmission loss of CPS electrodes is largely determined by the transverse resonance in the substrate, while the coupling between the fundamental coplanar waveguide mode and substrate mode has a stronger impact on CPW electrode loss [12].

In a previous study, we fabricated a coplanar microstrip line electrode to drive an EO polymer/TiO2 multilayer slot waveguide modulator and measured the DC half-wave voltage of the structure [5]. In this study, we analyzed the structure at high frequency and high speed. The optical response is the

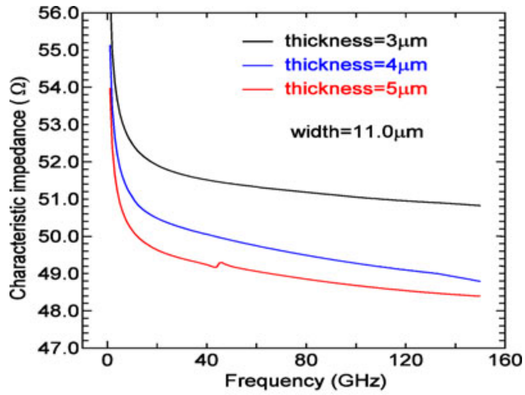

(a)

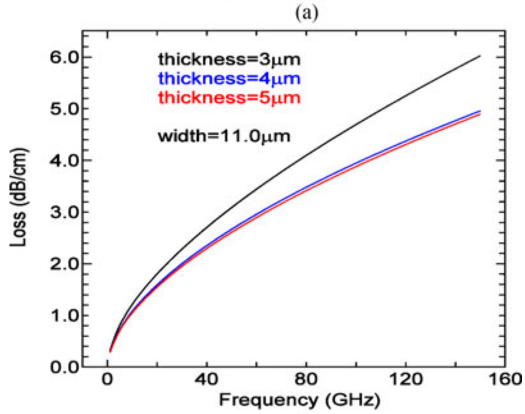

(b)

Fig. 2. (a) Characteristic impedance and (b) loss of microwave transmission line.

most directly informative parameter for the high-speed target, and the half-wave voltage decreases as optical response increases. Thus, it is inversely proportional to the optical response in high frequency [13]. FEM simulation results indicated that our traveling wave electrode can achieve an impendence of around 50 Ω, and that the 3-dB modulation bandwidth is mainly limited by velocity mismatch. Bandwidth over 200 GHz was achievable with an electrode of the proposed design 1 cm in length. For the sake of comparison, we also analyzed the EO polymer/Si multilayer slot waveguide modulator, which showed bandwidth of only 20 GHz at 3-dB modulation with transverse electric (TE) polarized light.

2. Proposed Structure

We first insert a TiO2 film layer into the electro-optic polymer multilayer waveguide MZ channel modulator. The structure's cross section is depicted in Fig. 1. A sol-gel silica was prepared for the waveguide cladding layers, then lower claddings 4 μm in thickness were coated on a 100-nm-thick Au lower electrode and silica (6 μm)-on-silicon substrate. A side cladding layer was spin-coated on the lower cladding to form a 4-μm-wide window for the EO polymer/TiO_2 multilayer slot core, and a 100-nm-thick TiO_2 layer was sputtered as a lower slot core layer between the etched sol-gel-side cladding layers on the lower cladding.

SEO125, which is a low-index EO polymer (1.621 index at 1550 nm), was spin-coated to create a 300-nm-thick layer after baking it overnight at 80° C in a vacuum oven [5]. A 100-nm-thick TiO_2 layer was then sputtered for the upper slot layer. The 500-nm-thick EO polymer/TiO_2 multilayer slot core was formed by side cladding to ensure effective mode confinement.

We completed the EO polymer poling, removed it, sputtered the upper slot layer, then coated Cytop (Asahi Glass) to 0.9-μm thickness as a buffer layer for the subsequent Au upper electrode

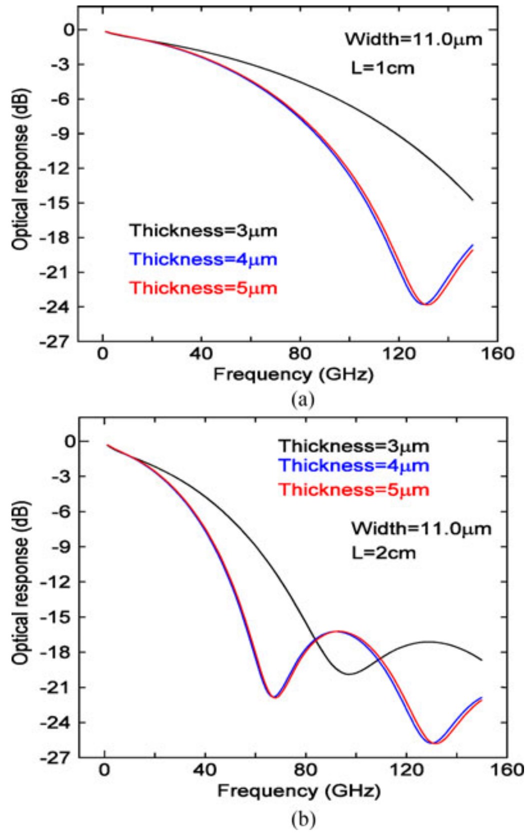

Fig. 3. Optical responses. (a) 1 cm electrode and TE polarized light. (b) 2 cm electrode and TE polarized light.

deposition. The optical indices of the sol-gel cladding, Cytop, and sputtered TiO_2 at 1550 nm were 1.487, 1.328, and 2.567, respectively, at 1550 nm.

The electrode and optical waveguide were placed in parallel arrangement and the modulating electrical wave and optical wave propagated along the same direction (Fig. 1). The two waves interact in a distributed manner; the optical wave is modulated by the electrical wave via EO effect. When the velocities of the two waves are equal (i.e., velocity-matched,) the wave front of the electrical wave and that of the optical wave depart the input simultaneously and propagate to the output without delay. The change in the electrical wave is transferred directly to the optical wave and, in theory, there is unrestricted modulation speed and bandwidth if the frequency-dependent electrode loss was ignored.

In actuality, the dielectric constants of the electrical and optical wave differ, as do their effective refractive indices. To this effect, the optical and electrical waves propagate at different velocities in the modulator. As the two waves progress, the separation between their wave fronts gradually increases and causes modulation efficiency degradation at higher frequencies, which restricts the modulation bandwidth.

3. Numerical Results and Discussion

Traveling-wave modulator modulation bandwidth is dependent on the microwave propagation characteristics of the electrode. Bandwidth-restricting factors include impedance mismatch between the driving circuit and electrode, velocity mismatch between the microwave and optical wave, and microwave propagation loss of the electrode.

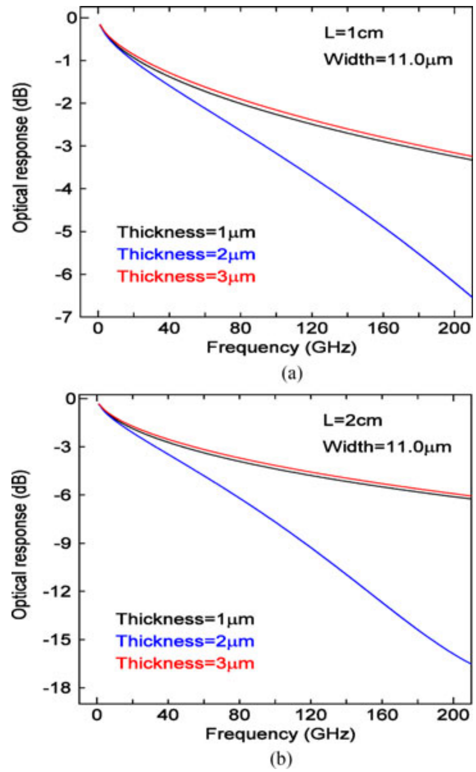

Fig. 4. Optical responses. (a) 1 cm electrode and TM polarized light. (b) 2 cm electrode and TM polarized light.

We eliminated the reflection wave effects by terminating the electrode with a load that had the same impedance as the electrode's characteristic impedance. This caused the microwave drive power requirements to increase and some of the available power from the source to be lost due to reflections originating from driver-electrode impedance mismatch. Because almost all microwave sources have 50 Ω output impedance, it was crucial to ensure the modulator electrode characteristic impedance was as closely matched to 50 as possible.

When the characteristic impedance of the traveling-wave modulator is matched to the driver and load, the small-signal modulation response can be expressed as follows [14]:

$$M(f) = e^{-\alpha l/2}\left[\frac{\sinh^2(\alpha l/2) + \sin^2(\xi l/2)}{(\alpha l/2)^2 + (\xi l/2)^2}\right] \tag{1}$$

where

$$\xi = 2\pi f(n_m - n_o)/c. \tag{2}$$

α and l are the microwave attenuation constant and electrode length, respectively. f is the microwave frequency, n_m is the microwave effective index, n_o is the optical effective index, and c is the light velocity in free space.

Equation (1) shows where a low-loss velocity and impedance-matched electrode are essential in establishing a wide-bandwidth traveling-wave modulator. A strong electric field that overlaps the optical mode and moves in the correct direction as-dictated by the electro-optic material is also a crucial requirement for the electrode, as it is necessary to reduce the drive voltage of the modulator.

The commercial software HFSS is used to simulate the traveling wave electrode. As mentioned above, the characteristic impedance of the structure was matched to 50 Ω to reduce reflection

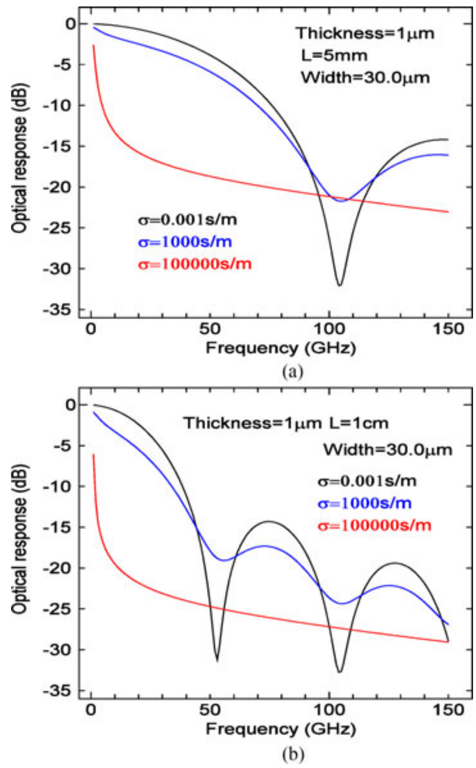

Fig. 5. Optical response of the silicon layer slot waveguide modulator structure. (a) 5 mm electrode. (b) 1 cm electrode.

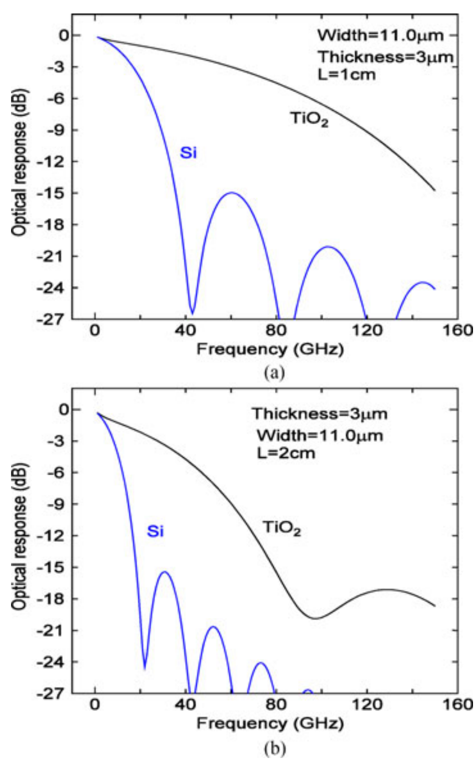

Fig. 6. Optical responses of silicon and TiO_2 layer slot waveguide modulators with TE polarized light. (a) 1 cm electrode. (b) 2 cm electrode.

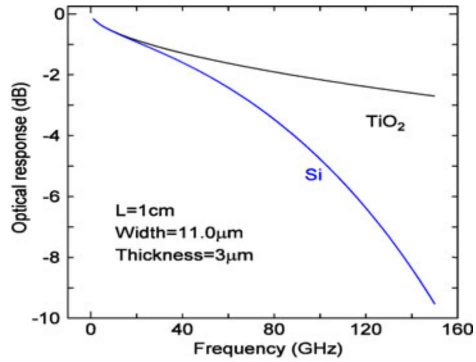

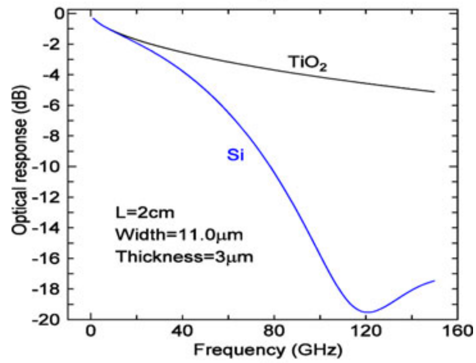

Fig. 7. Optical responses of silicon and TiO_2 layer slot waveguide modulators with TM polarized light. (a) 1 cm electrode. (b) 2 cm electrode.

and increase transmission efficiency. Fig. 2 shows the simulated characteristic impedance and loss curves of the microwave transmission line by the frequency function ranging from 1 GHz to 150 GHz as electrode thickness varied from 3 to 5μm at the width 11 μm; the characteristic impedance curves dropped to 50 Ω, and the loss curves decreased as thickness increased from 3 to 5 μm. Especially between 3 μm and 4 μm, the difference was quite large compared to that between 4 μm and 5 μm, because loss is affected considerably by metal thickness and skin depth. For subsequent analysis, we selected relative permittivity of TiO_2 of 30.

The optical effectiveness indices of the multilayer optical waveguides were obtained by Fourier series expansion method. We expanded the electric and magnetic fields in a Fourier series via complex trigonometric functions to reduce the Maxwell's equations to an eigenvalue problem comprised of a set of linear equations for Fourier coefficients. (This method has proven effective for many other optical waveguide problems [13].) In our model, optical effective indices were calculated as 1.804 and 1.600 for TE and TM polarized light at 1550 nm, respectively.

Per (1), we found that the optical response for TE and TM polarized light along the electronic frequency at the 1-cm and 2-cm long electrodes are shown in Figs. 3 and 4. The response declined in quality as electrode length increased, as expected based on (1). Remarkably, though, the best 3-dB bandwidth was very high – over 200 GHz – for TM polarized light with thickness of 3 μm and a 1 cm electrode. The same target dropped to around 60 GHz for TE polarized light with 3 μm thickness, however, because the optical response can be approximately $1.9c/(\pi|n_m - n_o|l)$ if the electronic loss is neglected [16]. In other words, the difference in electronic and optical effective index is a critical factor of optical response compared to electronic loss (regardless of electrode length).

Silicon, the semiconductor material of choice for most microelectronics engineers, is also typically used to create photonic integrated circuits. There is attractive potential in integrating photonics with mainstream electronics and silicon technology, as successfully doing so may enable integrated optics to be fabricated conveniently and economically.

We replaced the TiO2 layers with silicon layers in the same slot waveguide modulator structure to conduct a comparative experiment. Because silicon is a semiconductor material, its conductivity fluctuates widely (10^{-4} to 10^5 s/m) with different doping concentrations. Three different conductivities (10^{-3}, 10^3, and 10^5 s/m) of doping silicon were selected and plugged into the numerical model with metal thickness of 1 μm, width of 30 μm, and lengths of 5 mm and 1 cm. The optical response curves gradually decreased as conductivity increased, as shown in Fig. 5. The 3-dB bandwidth narrowed mostly due to material loss in the structure with silicon.

In addition, we found that replacing the TiO_2 layers with even no doping silicon, the silicon layer slot waveguide's optical effective indices were 2.293 (TE polarized light) and 1.681 (TM polarized light), which created sizable difference between the electronic and optical effective indices as well as heavy velocity mismatch and caused the 3-dB bandwidth to narrow all the way down to 20 GHz (TE), 70 GHz (TM) and 10 GHz (TE), 30 GHz (TM) at 1 cm and 2 cm electrode lengths, as shown in Figs. 6 and 7, respectively.

Taken together, our simulation results suggested that the TiO2 layer is better suited to a high-performing slot waveguide modulator than a silicon layer.

4. Conclusion

In this study, we built a traveling wave electrode and used it to drive a high-speed EO polymer/TiO_2 multilayer slot waveguide modulator. We tested the performance of this setup via simulation experiments. The electrode on top of the active region and the connection transmission line were optimized to match the impedance at 50 Ω. The 3-dB bandwidth reached over 200 GHz for TM polarized light with thickness of 3 μm at the 1-cm-long electrode. When the TiO2 layer was replaced with silicon in the same modulator, optical response dropped to 20 GHz at the same length of electrode with TE polarized light. In short, TiO2 performs better than silicon in terms of high-speed performance criteria for slot waveguide modulators.

References

[1] D. Chen *et al.*, "Demonstration of 110 GHz electrooptic polymer modulator," *Appl. Phys. Lett.*, vol. 70, no. 25, pp. 3335–3337, 1997.

[2] D. Chen *et al.*, "High frequency polymer modulators with integrated finline transitions and low V_π," *IEEE Photon. Technol. Lett.*, vol. 11, no. 1, pp. 54–56, Jan. 1999.

[3] Y. Enami *et al.*, "Hybrid electro-optic polymer/sol-gel waveguide directional coupler switches," *Nature Photon.*, vol. 1, pp. 180–185, Mar. 2007.

[4] M. Gould *et al.*, "Silicon-polymer hybrid slot waveguide ring-resonator modulator," *Opt. Exp.*, vol. 19, no. 5, pp. 3952–3961, 2011.

[5] Y. Enami, B. Yuan, M. Tanaka, J. Luo, and A. K.-Y. Jen, "Electro-optic polymer/TiO2 multilayer slot waveguide modulators," *Appl. Phys. Lett.*, vol. 101, 2012, Art. no. 123509.

[6] Y. Enami, Y. Jouane, D. Zhang, Y. Chang, J. Luo, and A. Jen, "Hybrid electro-optic polymer/TiO2 multilayer slot waveguide modulators for lower half wave voltage and electrode length product," in *Proc. Frontiers Opt., OSA Tech. Dig. Online*, 2014, Paper FW5B.5.

[7] K. Noguchi, O. Mitomi, H. Miyazawa, and S. Seki, "A broad band Ti:LiNbO3 optical modulators with a ridge structure," *J. Lightw. Technol.*, vol. 13, pp. 1164–1168, Jun. 1995.

[8] D. G. Girton, S. L. Kwiatkowski, G. F. Lipscomb, and R. S. Lytel, "20 GHz electro-optic polymer mach zehnder modulator," *Appl. Phys. Lett.*, vol. 58, no. 16, pp. 1730–1732, Apr. 1991.

[9] C. C. Teng, "Traveling–wave polymeric optical intensity modulator with more than 40 GHz of 3-dB electrical bandwidth," *Appl. Phys. Lett.*, vol. 60, no. 13, pp. 1538–1540, Mar. 1992.

[10] M.-C. Oh *et al.*, "Recent advances in electro-optic polymer modulators incorporating phenyltetracene bridged chromophores," *IEEE J. Sel. Topics Quantum Electron.*, vol. 7, no. 5, pp. 826–835, Sep. 2001.

[11] K. Noguchi, H. Miyazawa, and O. Mitomi, "Frequency dependent propagation characteristics of coplanar waveguide electrode on 100 GHz TiLiNbO3 optical modulator," *Electron. Lett.*, vol. 34, no. 7, pp. 661–663, Jan. 28, 1998.

[12] G. K. Gopalakrishnan, W. K. Burns, and C. H. Bulmer, "Electrical loss mechanism in traveling wave switch/modulators," *Electron. Lett.*, vol. 28, no. 2, pp. 207–209, 1992.

[13] Z. Liu and D. Zhu, "The effect of conductor loss on half-wave voltage and modulation bandwidth of electro-optic modulators," *Chin. Opt. Lett.*, vol. 2, no. 10, pp. 586–589, 2004.

[14] N. Dagli, “Wide bandwidth lasers and modulators for RF photonics,” *IEEE Trans. Microw. Theory Techn.*, vol. 47, no. 7, pp. 1151–1171, Jul. 1999.
[15] D. Zhang and H. T. Jia, “Numerical analysis of leaky modes in two-dimensional photonic crystal waveguides using fourier series expansion method with perfectly matched layer,” *IEEE Trans. Electron.*, vol. E90-C, no. 3, pp. 613–622, Mar. 2007.
[16] M. Izutsu, Y. Yamane, and T. Sueta, “Broad-band traveling-wave modulator using a LiNbO3 optical waveguide,” *IEEE J. Quantum Electron.*, vol. QE-13, no. 4, pp. 287–290, Apr. 1977.